

# 1 Utility of nasal swabs for assessing mucosal immune responses towards SARS- 2 CoV-2

3 Ericka Kirkpatrick Roubidoux<sup>1</sup>, Pamela H. Brigleb<sup>1</sup>, Kasi Vegesana<sup>2</sup>, Aisha Souquette<sup>2</sup>, Kendall Whitt<sup>1</sup>,  
4 Pamela Freiden<sup>1</sup>, St. Jude Investigative Team<sup>†</sup>, Amanda Green<sup>2</sup>, Paul G. Thomas<sup>2</sup>, Maureen A. McGargill<sup>2</sup>,  
5 Joshua Wolf<sup>1</sup>, Stacey Schultz-Cherry<sup>1\*</sup>

6 <sup>1</sup>Department of Infectious Diseases, St. Jude Children's Research Hospital, Memphis, Tennessee, USA

7 <sup>2</sup>Department of Immunology, St. Jude Children's Research Hospital, Memphis, Tennessee, USA

8

9 <sup>†</sup>The members of the St. Jude Investigative Team are as follows:

10 Kim J. Allison<sup>1</sup>, Sean Cherry<sup>1</sup>, Ronald H. Dallas<sup>1</sup>, Aditya H. Gaur<sup>1</sup>, Ashleigh Gowen<sup>1</sup>, Hana Hakim<sup>1</sup>, Diego R.  
11 Hijano<sup>1</sup>, Jamie Russell-Bell<sup>1</sup>, Elaine I. Tuomanen<sup>1</sup>, and Richard J. Webby<sup>1</sup>, E. Kaitlynn Allen<sup>2</sup>, Walid Awad<sup>2</sup>,  
12 Resha Bajracharya<sup>2</sup>, David C. Brice<sup>2</sup>, Ashley Castellaw<sup>2</sup>, Allison M. Kirk<sup>2</sup>, Chun-Yang Lin<sup>2</sup>, Robert C.  
13 Mettelman<sup>2</sup>, Lee-Ann Van de Velde<sup>2</sup>, and Taylor L Wilson<sup>2</sup>, James Hoffman<sup>3</sup>, Randall T. Hayden<sup>4</sup>

14 <sup>1</sup>Department of Infectious Diseases, St. Jude Children's Research Hospital, Memphis, Tennessee, USA

15 <sup>2</sup>Department of Immunology, St. Jude Children's Research Hospital, Memphis, Tennessee, USA

16 <sup>3</sup>Office of Quality and Patient Care, St. Jude Children's Research Hospital, Memphis, TN, USA

17 <sup>4</sup>Department of Pathology, St. Jude Children's Research Hospital, Memphis, TN, USA

18

19 \*Corresponding author: [stacey.schultz-cherry@stjude.org](mailto:stacey.schultz-cherry@stjude.org)

## 20 Abstract

21 SARS-CoV-2 has caused millions of infections worldwide since its emergence in 2019. Understanding how  
22 infection and vaccination induce mucosal immune responses and how they fluctuate over time is  
23 important, especially since they are key in preventing infection and reducing disease severity. We  
24 established a novel methodology for assessing SARS-CoV-2 cytokine and antibody responses at the nasal  
25 epithelium by using nasopharyngeal swabs collected longitudinally before and after either SARS-CoV-2  
26 infection or vaccination. We then compared responses between mucosal and systemic compartments.  
27 We demonstrate that cytokine and antibody profiles differ markedly between compartments. Nasal  
28 cytokines show a wound healing phenotype while plasma cytokines are consistent with pro-inflammatory  
29 pathways. We found that nasal IgA and IgG have different kinetics after infection, with IgA peaking first.  
30 Although vaccination results in low nasal IgA, IgG induction persists for up to 180 days post-vaccination.

31 This research highlights the importance of studying mucosal responses in addition to systemic responses  
32 to respiratory infections to understand the correlates of disease severity and immune memory. The  
33 methods described herein can be used to further mucosal vaccine development by giving us a better  
34 understanding of immunity at the nasal epithelium providing a simpler, alternative clinical practice to  
35 studying mucosal responses to infection.

36

## 37 **Teaser**

38 A nasopharyngeal swab can be used to study the intranasal immune response and yields much more  
39 information than a simple viral diagnosis.

## 40 **Introduction**

41 In 2019, the SARS-2 coronavirus (SARS-CoV-2) pandemic began in Wuhan, China and quickly spread across  
42 the globe. The primary route of infection with SARS-CoV-2 is through the inhalation of respiratory  
43 droplets, with infections typically beginning at the mucosal surface of the nasal cavity<sup>1,2</sup>. The spike protein  
44 is responsible for viral entry via the angiotensin-converting enzyme 2 (ACE2) receptor on nasal epithelial  
45 cells<sup>2</sup>. It is also the target of antibody responses, with those targeting the receptor binding domain (RBD)  
46 being the most neutralizing<sup>3,4</sup>. Shortly after infection, antibodies towards the RBD arise with IgA and IgG  
47 detectable around 9 days post-infection<sup>5</sup>.

48 Immunoassays have been developed as tools to study immune responses to infection and vaccination,  
49 however, they are focused on serological reactions to the virus. Serological assays are important and have  
50 aided in our understanding of anti-SARS-CoV-2 immunity and supported the development of SARS-CoV-2  
51 vaccines. It is understood that the immune response can be compartmentalized, with mucosal responses  
52 differing from systemic<sup>6,7</sup>. Additionally, mucosal immunity within the upper respiratory tract (URT) is a key  
53 factor in preventing and controlling infections<sup>8-11</sup>. Typically, saliva or nasal washes are collected as  
54 representative samples of the URT mucosal compartment. These types of samples do capture secretions  
55 from mucosal surfaces; however, they come with some caveats. Nasal washes are highly invasive, leading  
56 to participant hesitancy. Saliva is a non-invasive sample type, but saliva is not representative of the nasal  
57 mucosa, and its proximity to the gingiva can lead to a more intermediate phenotype between a mucosal  
58 and systemic sample<sup>12</sup>. The large volumes collected may also dilute the signal, and most studies do not  
59 control sample-to-sample variability. Finally, no studies to date have examined the longitudinal kinetics  
60 of nasal responses toward SARS-CoV-2.

61 To fill this gap in knowledge and further our understanding of innate and humoral immunity towards  
62 SARS-CoV-2 in the nasal cavity, we designed a series of experiments to measure cytokines and antibodies  
63 in nasopharyngeal (nasal) swabs collected longitudinally from individuals enrolled in our St. Jude Tracking  
64 of Viral and Host Factors Associated with COVID-19 (SJTRC) cohort study<sup>13</sup>. Participants were swabbed  
65 weekly in an institutional surveillance program to screen for SARS-CoV-2 infections. Nasal swabs were  
66 available from the baseline (pre-infection), acute, early convalescent, late convalescent, post  
67 convalescent, and late post convalescent phases of COVID-19 disease. After the release of the BNT162b2  
68 (Pfizer) mRNA vaccines in late 2020, participants were offered vaccinations, providing an opportunity to  
69 measure nasal antibodies after vaccination. To determine the differences between nasal and systemic  
70 responses, cytokine and antibody levels were quantitated over time from the same participants. Our  
71 studies uncovered that longitudinal kinetics vary depending on infection or vaccination, antibody isotype,  
72 and viral antigen. We also noted that the mucosal and systemic responses are compartmentalized and  
73 have distinct profiles that persist long after infection or vaccination. Importantly, our work highlights that  
74 nasal swabs are a powerful, underutilized tool for further understanding nasal mucosal immunity.

## 75 **Results**

### 76 **Study design and sample collection**

77 Nasal swabs were collected weekly from participants enrolled in the SJTRC cohort study for asymptomatic  
78 monitoring and after infection to document clearance. We selected 48 individuals with RT-PCR confirmed  
79 SARS-CoV-2 infection (CT value < 40) and 26 vaccinated individuals (BNT162b2 [Pfizer] mRNA vaccination,  
80 2 doses, three weeks apart) for these studies. Cohort characteristics are described in **Table 1**. Most  
81 infections were caused by SARS-CoV-2 B.1 lineage viruses and no severe illness was reported. Nasal swabs  
82 and a plasma sample were collected pre-exposure (baseline), and during the acute (1-21 days post  
83 infection, dpi), early convalescent (22-59 dpi), late convalescent (60-89 dpi), post convalescent (90-180  
84 dpi), and late post convalescent (>180 dpi) phases of infection (**Fig. 1**). Additionally, nasal swabs and  
85 plasma were available from vaccinated individuals prior to vaccination and then during the 22-56 days  
86 post vaccination (dpv), 57-89 dpv, 90-180 dpv, and >180 dpv periods. None of the included vaccinated  
87 individuals were diagnosed with SARS-CoV-2 during this period. This study design provided us with an  
88 opportunity to investigate mucosal cytokine and antibody responses longitudinally compared to pre-  
89 exposure levels. The collection of baseline nasal swabs and plasma is unique to this study and enabled us  
90 to make better inferences with the data, since baseline immune responses can vary amongst people.

91 Nasal swab quality was assessed using RNase P qPCR. All nasal swabs with a Ct value below 40 were  
92 included in the study. Nasal swabs were then handled as depicted in **Figure 2**. To reduce swab-to-swab  
93 variability, total protein concentration was determined, and nasal swab material was diluted to a protein  
94 concentration of 0.5 mg/mL for subsequent assays. These steps ensured that each nasal swab was  
95 standardized for downstream experiments and allowed for more direct comparisons between samples.  
96 We then used these nasal swabs to assess longitudinal nasal cytokine and antibody kinetics in our infected  
97 and vaccinated cohorts.

### 98 **Cytokine and chemokine responses are distinct between nasal and systemic compartments**

99 Cytokine levels are commonly assessed in the blood to determine systemic levels of inflammation. Prior  
100 studies, including one from this cohort<sup>14</sup>, have shown elevated systemic levels of specific cytokines,  
101 including IL-1Ra and IL-8, have been previously associated with an increased risk of severe disease and  
102 poor outcomes in persons with SARS-CoV-2 infection<sup>15–18</sup>. However, little is known about the mucosal  
103 immune response to SARS-CoV-2 infection and whether the mucosal immune responses correlate with  
104 systemic immune responses, especially at later time points. These are important to understand the long-  
105 term impact of an upper-lower respiratory infection on mucosal immunity that may impact the  
106 susceptibility and severity to other respiratory infections. In this study, both mucosal (nasal) and systemic  
107 (plasma) immunity to natural SARS-CoV-2 infection were assessed by multiplex Luminex analysis to  
108 determine the levels of 31 different cytokines/chemokines. Since baseline levels differed (**Supplementary**  
109 **Fig. 1**), each acute or convalescent time point was normalized to their baseline.

110 Several plasma cytokines had an increased fold change following infection with the most robust increases  
111 observed with CXCL10, TNF $\alpha$ , IL-10, and IL-1RA, corroborating previously published data<sup>19–22</sup>. To  
112 investigate whether mucosal immune responses would trend similarly to systemic responses, we used a  
113 similar Luminex Cytokine Human Panel on nasal swab samples diluted to 0.5 mg/ml. Although we detected  
114 a smaller percentage of cytokines in the nasal swabs compared to the plasma, 12/30 compared to 30/30  
115 in the plasma (**Fig. 3A & 3B**), there was an opposite trend to that observed in the plasma. Instead of the  
116 overall increase in cytokines seen in the plasma, we observed a decrease in several cytokine levels at the  
117 acute time point in the nasal swabs, including CCL2, IL1-RA, and IL-8, which were elevated in the plasma  
118 in the acute stage. This suggests that inflammatory immune responses are more concentrated  
119 systemically as the infection has migrated to other sites of infection (e.g., lungs or gastrointestinal tract)  
120 at those time points. Ingenuity pathway analysis of the cytokines up or down-regulated in the nasal swabs

121 were consistent with a wound healing phenotype while those in the plasma with pathogen-induced  
122 inflammatory signaling pathways (**Fig. 3A & 3B**).

123 One strength of these studies is the availability of longitudinal samples, allowing us to assess the impact  
124 of infection and vaccination on long-term systemic and mucosal immune responses. While no significant  
125 differences were observed in the plasma (**Fig. 3D**), we found that there were still changes in cytokine  
126 expression in the nasal cavity weeks following infection. In our early convalescent timepoint, there were  
127 several cytokines that were upregulated including FGF and IL2R (**Fig. 3B and 3D**). In late convalescence,  
128 we found that most cytokines were still downregulated in the nasal cavity, including IL-1RA, IL-8, and VEGF  
129 (**Fig. 3B and 3D**). These data suggest that infection with SARS-CoV-2 may alter cytokine responses,  
130 specifically at the mucosal surface, long term, which may have implications in reinfection and  
131 susceptibility to other respiratory infections.

### 132 **Development of high-throughput methodology for characterizing longitudinal mucosal antibody** 133 **responses using nasal swab**

134 After observing the stark differences between cytokine and chemokine expression in nasal and systemic  
135 compartments, we next wanted to evaluate whether they translated to differences in antibody  
136 expression. Also, it is important to understand how nasal antibody levels rise and fall after SARS-CoV-2  
137 exposure or vaccination to determine the longevity of memory immune responses. To do this, we mapped  
138 the longitudinal nasal responses of both infected and vaccinated SJTRC participants as depicted in **Fig. 2**.  
139 Total IgA and IgG present in each nasal swab was measured using an enzyme-linked immunosorbent assay  
140 (ELISA). Area under the curve (AUC) analyses were performed and used as the value for total IgA or IgG.  
141 SARS-CoV-2 RBD and N-specific antibodies were detected using a multiplex Luminex assay, and the  
142 average mean fluorescent intensity (MFI) for each sample was reported. Baseline nasal swabs were used  
143 to establish background signal. To normalize the levels of SARS-CoV-2 specific antibodies in proportion to  
144 total IgA or IgG present in a sample, we calculated a positivity ratio of antigen-specific IgA or IgG to total  
145 IgA or IgG.

146 Importantly, we were able to confidently detect SARS-CoV-2 specific IgA and IgG at the nasal epithelium  
147 using nasal swabs. Within the infected cohort, anti-RBD and -N IgA titers peak early after infection and  
148 then steadily decline (**Fig. 4**). Anti-RBD and -N IgG titers rise and remain at moderate levels for an extended  
149 period. In most cases, anti-RBD and N antibodies return to baseline levels by late post-convalescence. The  
150 exception is anti-RBD IgG titers, which increase between the post convalescence and late post

151 convalescence phases for several individuals. These individuals had received their first dose of the  
152 BNT162b2 mRNA vaccine in the intervening period, which explains the discrepancy. Of note, they are not  
153 included in the vaccinated cohort.

154 Within the vaccinated cohort, we observed a small peak of anti-RBD IgA at 22-56 dpv (**Fig. 4**). On average,  
155 this peak was half of the response observed for the corresponding time post infection (early  
156 convalescence). Their levels return to baseline by 57-89 dpv. Anti-RBD IgG titers rose to similar levels as  
157 infected individuals and remained stable for up to 180 dpv. As expected, anti-N titers were negligible.  
158 Infection leads to an IgA and IgG response to both SARS-CoV-2 antigens evaluated while vaccination  
159 appears to only induce a strong anti-RBD IgG response.

160 Using cohort data previously collected about the plasma response to SARS-CoV-2<sup>23-25</sup>, we mapped the  
161 matched plasma antibody levels of participants (**Supplemental Fig. 2**) and observed that IgA antibody  
162 kinetics between the compartments are different, with IgA peaking during early convalescence in plasma.  
163 Additionally, IgA responses seem to last longer in plasma from both infected and vaccinated participants.  
164 IgG responses were more uniform between the nasal and systemic compartments. This may be due to the  
165 mechanisms of IgA and IgG induction and transport since IgA is produced locally in the nasal cavity while  
166 IgG is bi-directionally transported between the two compartments<sup>26-28</sup>. This data highlight that the  
167 location and timing of sample collection could greatly impact the observed antibody response. Nasal  
168 responses are more readily detected after exposure, while systemic responses persist longer.

### 169 **Assessing the nasal swab neutralization activity**

170 Serological data show that neutralizing antibodies are a correlate for protection from SARS-CoV-2  
171 infection and severe disease<sup>3,4</sup>. Studies using other mucosal samples such as saliva and nasal washes have  
172 shown that antibodies in the URT can be neutralizing<sup>11,29,30</sup>. It is important to be able to detect and  
173 measure neutralization activity of antibodies at the nasal epithelium, especially since this is the primary  
174 site of infection. We chose nasal swabs with the top 10% anti-RBD IgA and IgG positivity ratios to assess  
175 whether neutralizing antibodies are detectable at the nasal epithelium using a SARS-CoV-2 spike VSV-ΔG-  
176 luciferase pseudovirus. We observed that nasal swabs from infected individuals had a higher average  
177 neutralizing activity compared to the vaccinated cohort (**Fig. 5**). Within the infected cohort there was a  
178 wider range of neutralizing capacity, with few nasal swabs completely neutralizing the virus. Only one  
179 nasal swab within the vaccinated cohort had elevated levels of neutralizing antibodies. This data suggests  
180 that while the quantity of anti-RBD IgG antibodies is similar between infected and vaccinated cohorts, the

181 quality is not. Upon further analysis, we noted that neutralizing nasal swabs had higher anti-RBD IgG  
182 positivity ratios compared to anti-RBD IgA positivity ratios, suggesting that neutralization is more IgG  
183 driven (**Supplemental Fig. 3 and Supplemental Table 1**). This is a consideration to make when evaluating  
184 new, mucosal vaccine responses as it will be important for them to induce long-lived IgG responses that  
185 are effectively trafficked to the nasal epithelium.

#### 186 **Longitudinal IgG responses do not exhibit compartmental bias**

187 Other studies, which used a variety of mucosal samples, have reported compartmental bias between  
188 mucosal and systemic compartments<sup>6,7,29,31,32</sup>. However, the comparison of longitudinal responses  
189 between nasal and systemic components has not yet been made. Within this study, data of antibody levels  
190 in the nasal cavity and plasma were collected differently (positivity ratio of antigen specific antibodies to  
191 total antibody levels vs ELISA determined optical density (OD) of antigen specific antibodies, respectively),  
192 making it difficult to directly compare responses between the compartments. We used a ranking system  
193 to compare whether an individual had a similar overall antibody response between both compartments.  
194 To do this, we calculated AUCs of the total nasal and plasma responses across all time points for each  
195 person within the study. We then ranked each positive individual from lowest to highest response and  
196 compared whether those with a high nasal rank also have a high plasma rank. Individuals with no response  
197 were given a rank of 0. We then graphed this data in a scatterplot and divided it into 4 quadrants: the top  
198 left represents those who had the highest 25% plasma responses, top right represents those who had the  
199 highest 25% of both plasma and nasal responses, bottom right represents those who had the highest 25%  
200 nasal responses, and the bottom left represents those who had the lowest 25% of both plasma and nasal  
201 responses (**Fig. 6**).

202 In all cases, most individuals fell into the lower left quadrant for both nasal and plasma responses. This  
203 may be because participants did not report any severe disease, which is known to induce a stronger  
204 antibody response<sup>33,34</sup>. A larger percentage of infected individuals ranked higher for plasma IgA than nasal  
205 IgA, regardless of antigen (**Fig. 6A-B**). This observation is driven by the fact that IgA persists longer in  
206 plasma, increasing the longitudinal AUC. Little IgA was observed in the vaccinated cohort; therefore, it is  
207 difficult to conclude whether the response was biased towards plasma or nasal responses. We observed  
208 better overall responses towards RBD compared to N, especially within IgA.

209 IgG responses had little compartmental bias, with the highest percentage of people ranking in the top  
210 25% of plasma and nasal responses (**Figure 6C-D**). Anti-RBD IgG responses ranked very similarly between



211 infected and vaccinated cohorts, which is corroborated by their comparable antibody kinetics. This data  
212 suggests that to get a complete picture of anti-SARS-CoV-2 IgA responses, both nasal and plasma  
213 compartments are important. However, overall responses to IgG are quite similar regardless of  
214 compartment or route of antigen exposure.

## 215 **Discussion**

216 This study demonstrates that nasal swabs can be used for more than diagnostic testing. By collecting  
217 baseline samples and standardizing nasal swab material, we established methodology that elucidated the  
218 longitudinal nasal anti-SARS-CoV-2 cytokine and antibody response. The data shown here highlights the  
219 importance of studying immunity at the infection site and systemically. The same pro-inflammatory  
220 cytokines upregulated systemically and were significantly downregulated at the nasal epithelium. The  
221 differences between nasal and systemic antibodies were less stark, however we did see that induction  
222 kinetics and longevity of IgA differ between compartments. The nasal response seems more short-lived  
223 compared to a plasma response. This is important to consider because the time of sample collection can  
224 play a role in influencing the levels of a respective antigen-isotype combination. Correlates for protection  
225 between nasal and systemic compartments will be vastly different depending on the timing and type of  
226 sample taken.

227 IgA seems to be more compartmentalized compared to IgG. The reasons behind this observation are both  
228 biologically and experimentally driven. First, IgA is produced in mucosal tissues and a secretory version is  
229 transported to mucosal surfaces through plg receptors, meaning that IgA is inherently more mucosal than  
230 IgG<sup>28,35,36</sup>. Additionally, IgA is more short-lived compared to IgG so there is a higher likelihood of IgG being  
231 detected at later time points regardless of compartment<sup>28,35,36</sup>. Other reasons for this observation can be  
232 due to experimental nuances. IgA quaternary structure is diverse and can be monomeric, dimeric,  
233 multimeric, or can contain a secretory signal (sIgA). The anti-human IgA secondaries used for this study  
234 may be biased towards plasma and not sIgA, making responses appear more compartmentalized than  
235 they really are. Interestingly, the extent of compartmental bias is different depending on longitudinal  
236 collection time highlighting the importance of long-term human cohort studies when investigating  
237 mucosal and systemic immunity.

238 We found that IgG kinetics were similar between infected and vaccinated cohorts regardless of bodily  
239 compartment. However, neutralizing IgG was only present in the infected cohort. This is important to note  
240 because it indicates that neutralizing antibodies induced by vaccination are not being trafficked to the



241 nasal epithelium. Our finding that neutralizing mucosal antibodies correlates with nasal IgG is unique.  
242 Other studies suggest that mucosal IgA is critical for neutralizing mucosal responses<sup>5,37,38</sup>. However, these  
243 studies used nasal washes or saliva as mucosal samples, and therefore are not measuring nasal  
244 epithelium. Our data suggests that IgA at the nasal epithelium is not playing as strong of a role in  
245 neutralization as IgA present in mucosal fluids. It underscores the importance of sample type when  
246 examining neutralizing mucosal responses. However, it should be noted that a luciferase-based  
247 pseudovirus platform is not as sensitive as some other SARS-CoV-2 neutralization assays and the use of  
248 live virus may increase the likelihood of identifying neutralizing IgA containing nasal swabs<sup>39</sup>.

249 We established the first study to examine longitudinal nasal antibody kinetics and confirmed existing  
250 reports of distinct cytokine responses. Additionally, longitudinal sampling revealed that SARS-CoV-2  
251 infection shifts the cytokine profile at the nasal epithelium and can take months to return to baseline  
252 levels, which may impact reinfection with SARS-CoV-2 or other respiratory pathogens. Finally, we  
253 uncovered important new information about nasal antibody kinetics that show compartmental bias can  
254 be observed at the antibody level as well. Kinetics differ between antibody isotype and site of collection,  
255 indicating that long term studies will provide the best information in terms of understanding the antibody  
256 response to SARS-CoV-2 as it is a very dynamic process. Infected individuals in our cohort reported mild  
257 to no clinical disease, which was reflected in their low antibody titers both mucosal and systemically. This  
258 additionally made it difficult to draw significant conclusions as to how the reported cytokine data  
259 influenced antibody outcomes. If studies using nasal swabs are continued in cohorts with stronger  
260 antibody responses, we may be able to use nasal swabs to detect biomarkers for poor disease outcomes  
261 or correlates of protection. Future work involving mucosal immunity should also consider investigating  
262 immunity within the nasal cavity as it gives a better picture of what is occurring at the site of infection  
263 compared to other mucosal samples. Additionally, nasal swabs are more ideal mucosal samples as they  
264 are sampling the correct anatomical location while being only mildly invasive.

## 265 **Methods**

### 266 **Study design and sample handling**

267 Participants in SJTRC provided written consent to participate in the institutional review-board approved,  
268 prospective study<sup>13</sup>. This study began with the collection of a blood sample (baseline), and the completion  
269 of a demographic survey, summarized in **Table 1**. As part of St. Jude COVID-19 employee surveillance,  
270 participants were swabbed weekly until staff vaccination became ubiquitous, and swabs collected prior

271 to diagnosis or vaccination were selected as baseline samples. Longitudinal nasal swabs and blood were  
272 collected after PCR-confirmed infection or after the second dose (“completion”) of the Pfizer mRNA  
273 BNT162b2 vaccine (**Fig. 1**). While nasal swabs and plasma were collected during the same time periods,  
274 they were not necessarily collected concurrently. Additionally, not all nasal swab samples have a matched  
275 plasma sample. Nasal swabs were collected using FLOQ Swabs (COPAN, Cat No. 520CS01) and placed in  
276 1mL of Viral Transport Media (DMEM with 0.25% FBS (Fetal Bovine Serum)) at 4°C and were stored at -  
277 80°C after collection. SARS-CoV-2 diagnostics were performed by the clinical microbiology laboratory at  
278 St. Jude the day of nasal swab collection. The remaining sample was kept at -80°C until received by our  
279 laboratory. Samples were thawed, RNA was immediately isolated, and remnants stored at 4°C for  
280 antibody and cytokine assays. Plasma was isolated from whole blood and stored at -80°C until needed for  
281 antibody and cytokine assays and kept at 4°C after thawed. Data are managed using an electronic  
282 database hosted at St. Jude (REDCap). The infected cohort consisted of 48 individuals and the vaccinated  
283 cohort consisted of 26 individuals.

#### 284 **RNase P qPCR**

285 Human nasal swab samples were inactivated with 350 µls RLT buffer (Qiagen, Cat No. 79216) containing  
286 1% β-mercaptoethanol for a minimum of 10 minutes. Following manufacturer’s recommended directions,  
287 RNA was extracted using a RNeasy Mini kit (Qiagen, Cat No. 74106) and assessed on a Nanodrop 2000.  
288 Four microliters of RNA were added to a 16ul master mix containing nuclease-free water (Teknova, Cat  
289 No. W3330), TaqMan Fast Virus 1-Step Master Mix (ThermoFisher, Cat No. 5555532) and a commercially  
290 prepared RNase P primer/probe combination (IDT, Cat Nos. 10006827, 10006828, 10007061, 10006829,  
291 10011568) to quality test for the human RNase P (RPP30) gene. A portion of the RPP30 gene was used as  
292 a positive control (IDT, Cat No. 10006626) and nuclease-free water was used as a negative control. A qRT-  
293 PCR assay was run on a BioRad CFX96 Real Time System with cycling conditions: 25°C for 2 mins, 50°C for  
294 15 mins, 95°C for 3 mins, followed by 45 rounds of 95°C for 15 secs, 55°C for 30 secs, data acquired. Ct  
295 values under 38 were considered positive. RNA extractions and qPCRs were performed in singlet. Only  
296 one nasal swab was removed from the study due to a high RNase P Ct value.

#### 297 **Measuring total protein**

298 The concentration of total protein in each nasal swab was determined using the Pierce™ BCA Protein  
299 Assay Kit (ThermoFisher, Cat No. 23225) according to the manufacturer’s microplate procedure. Briefly,  
300 neat nasal swab material and a 1:5 dilution of material in phosphate buffered saline (PBS) were added to

301 a clear, 96-well plate. Optical density (OD) at 562nm was read using BioTek Synergy2 plate reader and  
302 Gen5 (v3.09) software. All samples and standards were performed in duplicate, with averages used for  
303 calculations. Standard curve calculations were done in excel and concentrations were determined based  
304 on the average of both the neat and 1:5 dilution of nasal swab material, unless one of these values was  
305 out of the range used to determine the standard curve ( $>2\text{mg/mL}$  or  $<0.025\text{mg/mL}$ ). Once total protein  
306 concentrations were calculated, all nasal swabs were diluted to a standard concentration of  $0.5\text{mg/mL}$  in  
307 sterile 1xPBS and kept at  $4^{\circ}\text{C}$  for all downstream experiments.

### 308 **Cytokine and chemokine assays**

309 Cytokine levels were measured from plasma or nasal swab samples that included a baseline measurement  
310 per individual. Cohort plasma acute cytokine data were also used for a previous study<sup>14</sup>. Nasal swabs were  
311 pre-diluted to  $0.5\text{ mg/ml}$  for consistency with other protein analyses in this study. Cytokines were  
312 measured using the Human Cytokine Magnetic 30-Plex Panel (Invitrogen, Cat No. LHC6003M) and plates  
313 were read using a Luminex200 machine with xPONENT software (v4.3). Each sample was run in duplicate,  
314 and the average read was used for subsequent analyses. Sample exclusion from analyses included failure  
315 of detection for all cytokines and having no baseline value for comparison. Ingenuity pathway analysis  
316 (IPA) was used to identify pathways cytokines that were up or downregulated during the acute phase  
317 relative to baseline.

### 318 **Total IgA and IgG ELISAs**

319 Total IgA and IgG ELISAs were performed using 384-well flat-bottom MaxiSorp plates (ThermoFisher, Cat  
320 No. 464718) coated with either an unconjugated anti-human IgA (Novusbio, Cat No. NB7441) or an  
321 unconjugated anti-human IgG (Novusbio, Cat No NBP1-51523) antibody at  $2\mu\text{g}/\mu\text{L}$  in 1xPBS (**Fig. 2**). Once  
322 coated, plates were left overnight at  $4^{\circ}\text{C}$ . Plates were washed 4 times with PBS containing 0.1% Tween-  
323 20 (PBS-T) using the AquaMax 4000 plate washer system. After washing, plates were blocked with PBS-T  
324 containing 0.5% Omniblok non-fat milk powder (AmericanBio, Cat No. AB10109-01000) and 3% goat  
325 serum (Gibco, Cat No. 16210-072) for 1 hour at room temperature. The wash buffer was removed, and  
326 plates were tapped dry. Nasal swab material at  $0.5\text{mg/mL}$  was serially diluted 1:3 in blocking solution and  
327 run in duplicate. Recombinant human IgA (abcam, Cat No. ab91025) or recombinant human IgG (abcam,  
328 Cat No. ab91102) was also diluted to  $5\mu\text{g/mL}$  and ran in duplicate on each plate for quality control. D After  
329 2 hours at room temperature, plates were washed 4 times with PBS-T. Anti-human IgA HRP (Novusbio,  
330 Cat No NBP1-73613) diluted 1:2000 or anti-human IgG HRP (Creative Biolabs, Cat No. MOB-0361MC)

331 diluted 1:5000 was then added to the plates and left to incubate for 1 hour at room temperature. Plates  
332 were washed 4 times with PBS-T and developed using SIGMAFAST™ OPD (Sigma-Aldrich, Cat No. P9187)  
333 for 10 minutes at room temperature. The developing reagent was inactivated using 3M hydrochloric acid  
334 (Fisher Scientific, Cat No. A144-212). Plates were read at 490nm using a BioTek Synergy2 plate reader and  
335 Gen5 (v3.09) software. For each plate, an upper 99% confidence interval (CI) of blank wells OD values was  
336 determined and used as the Y= value in an area under the curve (AUC) analysis in PRISM 9. AUC was  
337 determined for each nasal swab and used as the denominator in positivity ratio calculations.

### 338 **IgA specific nasal antibodies**

339 SARS-CoV-2 anti-RBD and -N IgA antibody levels were determined using 2 kits due to a shortage of supplies  
340 while conducting experiments. To prevent kit-to-kit variability, samples were run concurrently on both  
341 kits and MFIs (Mean Fluorescent Intensity) were correlated. Additionally, positive control antibodies for  
342 RBD (InvivoGen, Cat No. srbd-mab6) and N (GenScript, Cat No. A02090) were included at high (30µg/mL)  
343 and low (0.01µg/mL) concentrations to each plate to monitor for plate-to-plate variability. We observed  
344 a strong correlation between MFI values for samples and control antibodies between the kits ( $r$  0.9951,  $p$   
345  $<0.0001$ ) (**Supplemental Fig. 4**). The first kit used was the Milliplex® SARS-CoV-2 antigen panel 1 IgA assay  
346 (Millipore Sigma, Cat No. HC19SERA1-85K) with the Wuhan-1 strain RBD and N proteins included. The  
347 second kit used was the Bio-Plex Pro Serology Reagent Kit (Bio-Rad, Cat No. 12014777), with human IgA  
348 positive and negative controls (Bio-Rad, Cat No. 12014775), Bio-Plex SARS-CoV-2 Wuhan-1 strain RBD and  
349 N coupled beads (Bio-Rad, Cat Nos. 12015406 and 12014773), and Bio-Plex Pro Human IgA detection  
350 antibody (Bio-Rad, Cat No. 12014669). For both kits, the manufacturers' instructions were followed,  
351 except that nasal swab material was diluted to 0.5mg/mL in PBS. The protocol for the Milliplex® SARS-  
352 CoV-2 kit involved incubating nasal swab material with RBD- and N- conjugated beads in the dark for 2  
353 hours at room temperature, shaking. The beads were then washed three times using a handheld magnetic  
354 separation block (EMD Millipore, Cat No. 40-285). Next, PE-anti-human IgA conjugate was added to each  
355 well and incubated in the dark for 90 minutes at room temperature, shaking. Beads were washed again  
356 three times and then resuspended in sheath fluid and stored at 4°C overnight, shielded from light. The  
357 protocol for the Bio-Plex kit involved incubating RBD- and N- conjugated beads with nasal swab material  
358 in the dark for 30 minutes at room temperature, shaking. Plates were washed 3 times using a handheld  
359 magnetic separation block and then human IgA detection antibody was added and incubated in the dark  
360 for 30 minutes, shaking. Next, plates were washed 3 times and SA-PE was added for 10 minutes, in the  
361 dark and shaking. Finally, beads were washed again three times and then resuspended in sheath fluid and

362 stored at 4°C overnight, shielded from light. The following day, plates were read using a Luminex200  
363 machine with xPONENT software (v4.3) and data was analyzed as “qualitative” using kit specific  
364 recommended plate layout and settings. All samples were measured in duplicate.

### 365 **IgG specific nasal antibodies**

366 SARS-CoV-2 anti-RBD and N IgG antibody levels were determined using the Milliplex® SARS-CoV-2 antigen  
367 panel 1 IgG assay (Millipore Sigma, Cat No. HC19SERG1-85K) with the Wuhan-1 strain RBD and N proteins  
368 included. The protocol was followed as described in the kit instructions, except that nasal swab material  
369 diluted to 0.5mg/mL in 1xPBS instead of assay buffer. Control antibodies for RBD (InvivoGen, Cat No. srbd-  
370 mab12) and N (AcroBiosystems, Cat No. NUN-S41) were added at high (30µg/mL) and low (0.01µg/mL)  
371 concentrations to each plate to monitor for plate-to-plate variability. Briefly, nasal swab material was  
372 incubated with RBD- and N- conjugated beads in the dark for 2 hours at room temperature, shaking. The  
373 beads were then washed three times using a handheld magnetic separation block. Next, PE-anti-human  
374 IgG conjugate was added to each well and incubated in the dark for 90 minutes at room temperature,  
375 shaking. Beads were washed again three times and then resuspended in sheath fluid and stored at 4°C  
376 overnight, shielded from light. Plates were read using a Luminex200 machine with xPONENT software  
377 (v4.3) and data was analyzed as “qualitative” using kit recommended plate layout and settings. All samples  
378 were measured in duplicate.

### 379 **Calculation of positivity ratios**

380 To account for non-specific signal from nasal swab material, we used baseline swabs to establish a  
381 positive/negative cutoff MFI for each antigen-isotype pair. All baseline MFI values for RBD IgA, RBD IgG,  
382 N IgA, and N IgG were individually averaged, and the top 99% confidence interval (3 standard deviations  
383 above the mean) was used as the antigen-isotype specific cutoff value. All MFIs below the cutoff value  
384 were given a negative value to ensure that only positive samples would have high positivity ratios. Next,  
385 the AUC of total IgA or total IgG for each nasal swab (determined via ELISA) was used as the denominator  
386 to calculate the positivity ratio (MFI/AUC). A positivity ratio of 1 or lower was considered negative.

### 387 **Determining plasma IgA and IgG antibodies**

388 Cohort plasma IgA and IgG antibodies were determined using an ELISA and used for previous studies<sup>23–25</sup>.  
389 Briefly, plates were coated with 1.5µg/mL of Wuhan-1 RBD or 1µg/mL Wuhan-1 nucleoprotein (produced  
390 in-house) and left overnight at 4°C. Next, plates were blocked with 3% milk in PBS-T for 1 hour at room  
391 temperature. Plates were washed three times and a 1:50 dilution of plasma in 1% milk was added to the

392 plate for 1.5 hours at room temperature. Next anti-human IgA HRP (Novusbio, Cat No. NBP1-73613)  
393 diluted 1:2000 or anti-human IgG HRP (Creative Biolabs, Cat No. MOB-0361MC) diluted 1:10,000 was  
394 added for 30 minutes at room temperature. Plates were washed again and developed using SIGMAFAST™  
395 OPD (Sigma-Aldrich, Cat No. P9187) for 8 minutes at room temperature and then stopped using 3M  
396 hydrochloric acid (Fisher Scientific, Cat No. A144-212). Plates were read at 490nm using a BioTek Synergy2  
397 plate reader and Gen5 (v3.09) software. OD was reported and anything 2-fold above negative control  
398 plasma (OD 0.15) was considered positive. Plasma samples were tested in duplicate.

### 399 **Neutralization Assays**

400 Neutralization assays were performed using a SARS-CoV-2 spike VSV-ΔG- luciferase pseudovirus that was  
401 generated as previously described<sup>39</sup>. Approximately 24 hours prior to the assay, VeroE6/TMPRSS2 cells  
402 (XenoTech, Cat No. JCRB1819) were plated at  $2.5 \times 10^4$  cells per well in a clear, 96-well tissue culture treated  
403 plate in DMEM (Corning, Cat No. 10-013-CV) supplemented with 5% FBS (Sigma, Cat No. F2442) (D-5). The  
404 following day, nasal swab material was diluted in D-5 media to 0.5mg/mL. The SARS-CoV-2 spike VSV-ΔG-  
405 luciferase pseudovirus was diluted to 250 infectious units (IU) and this was incubated with nasal swab  
406 material for 1 hour at 37°C in 5% CO<sub>2</sub>. The VeroE6/TMPRSS2 cells were then washed 1 time with 1xPBS  
407 and the virus+swab material mixture was immediately added. Plates were placed at 37°C in 5% CO<sub>2</sub> and  
408 left for 16-18 hours (overnight). The following day, Luc-Screen™ Extended-Glow Luciferase buffers 1 and  
409 2 (ThermoFisher, Cat No. T1035) used according to manufacturer's instructions. Luminescence was  
410 measured using the BioTek Cytation3 plate reader with 1 sec integration time and analyzed with Gen5  
411 (v3.09) software. Percent neutralization was calculated using the following equation:  $\left(100 - \frac{(\text{Nasal swab value} - \text{cell only average})}{(\text{Virus only average} - \text{cell only average})}\right) * 100$ . Virus only and cell only averages were calculated for each  
412 plate individually. As a control, a neutralizing monoclonal antibody towards SARS-CoV-2 (SinoBiologicals,  
413 Cat No. 40592-R0004) was included on each plate. All samples were run in duplicate. Percent  
414 neutralization, IgA positivity ratio, and IgG positivity ratio of each nasal swab tested are listed in  
415 **Supplemental Table 1.**

### 417 **Statistical analysis**

418 Data was managed using the software REDCap and visualized using R or PRISM 9.0. For cytokine and  
419 chemokine analyses, heat maps and subsequent statistical analyses were conducted in GraphPad Prism  
420 version 9 as described in figure legends. Statistical analyses include a One-way ANOVA with Tukey's  
421 Multiple Comparisons test. For the neutralization data, outliers were identified using the ROUT test and

422 significant differences between groups were detected using a Kruskal-Wallis multiple comparisons (with  
423 standard parameters) test in PRISM 9.0 as described in figure legends.

## 424 **Acknowledgements**

425 We would like to thank all SJTRC participants for their invaluable contribution to this study. Additionally,  
426 we would like to thank the staff of St. Jude Children’s Research Hospital and Lauren Rowland for their  
427 contributions.

## 428 **Funding**

429 This study was supported by American Lebanese Syrian Associated Charities (ALSAC) and St. Jude  
430 Children’s Research Hospital, the NIAID (National Institute of Allergy and Infectious Diseases)  
431 Collaborative Influenza Vaccine Innovation Centers (CIVIC) contract 75N93019C00052, NIAID grant  
432 3U01AI144616–02S1 to P.T., M.A.M., and S.S.C., and the NIH (National Institutes of Health) funded St.  
433 Jude Children’s Research Hospital Department of Infectious Disease T32 Training Grant T32AI106700-07  
434 to E.K.R.

## 435 **References**

- 436 1. V’kovski, P., Kratzel, A., Steiner, S., Stalder, H. & Thiel, V. Coronavirus biology and replication:  
437 implications for SARS-CoV-2. *Nat. Rev. Microbiol.* **19**, 155–170 (2021).
- 438 2. Ziegler, C. G. K. *et al.* SARS-CoV-2 Receptor ACE2 Is an Interferon-Stimulated Gene in Human  
439 Airway Epithelial Cells and Is Detected in Specific Cell Subsets across Tissues. *Cell* **181**, 1016-1035.e19  
440 (2020).
- 441 3. Goldblatt, D., Alter, G., Crotty, S. & Plotkin, S. A. Correlates of protection against SARS-CoV-2  
442 infection and COVID-19 disease. *Immunol. Rev.* **310**, 6–26 (2022).
- 443 4. Earle, K. A. *et al.* Evidence for antibody as a protective correlate for COVID-19 vaccines. *Vaccine*  
444 **39**, 4423–4428 (2021).
- 445 5. Patil, H. P. *et al.* Antibody (IgA, IgG, and IgG Subtype) Responses to SARS-CoV-2 in Severe and  
446 Nonsevere COVID-19 Patients. *Viral Immunol.* **34**, 201–209 (2021).
- 447 6. Smith, N. *et al.* Distinct systemic and mucosal immune responses during acute SARS-CoV-2  
448 infection. *Nat. Immunol.* **22**, 1428–1439 (2021).
- 449 7. Butler, S. E. *et al.* Distinct Features and Functions of Systemic and Mucosal Humoral Immunity  
450 Among SARS-CoV-2 Convalescent Individuals. *Front. Immunol.* **11**, (2021).
- 451 8. Holmgren, J. & Czerkinsky, C. Mucosal immunity and vaccines. *Nat. Med.* **11**, S45–S53 (2005).



- 452 9. Pearson, C. F., Jeffery, R. & Thornton, E. E. Mucosal immune responses in COVID19 - a living  
453 review. *Oxf. Open Immunol.* **2**, iqab002 (2021).
- 454 10. Russell, M. W., Moldoveanu, Z., Ogra, P. L. & Mestecky, J. Mucosal Immunity in COVID-19: A  
455 Neglected but Critical Aspect of SARS-CoV-2 Infection. *Front. Immunol.* **11**, (2020).
- 456 11. Fröberg, J. & Diavatopoulos, D. A. Mucosal immunity to severe acute respiratory syndrome  
457 coronavirus 2 infection. *Curr. Opin. Infect. Dis.* **34**, 181–186 (2021).
- 458 12. Brandtzaeg, P. Secretory immunity with special reference to the oral cavity. *J. Oral Microbiol.* **5**,  
459 20401 (2013).
- 460 13. St. Jude Children’s Research Hospital. *SJTRC-St. Jude Tracking of Viral and Host Factors Associated*  
461 *With COVID-19: A Prospective Adaptive Cohort Study*. <https://clinicaltrials.gov/ct2/show/NCT04362995>  
462 (2022).
- 463 14. Souquette, A. *et al.* Establishing thresholds for cytokine storm and defining their relationship to  
464 disease severity in respiratory viral infections. 2023.07.06.548022 Preprint at  
465 <https://doi.org/10.1101/2023.07.06.548022> (2023).
- 466 15. Zanza, C. *et al.* Cytokine Storm in COVID-19: Immunopathogenesis and Therapy. *Medicina (Mex.)*  
467 **58**, 144 (2022).
- 468 16. Nikkhoo, B. *et al.* Elevated interleukin (IL)-6 as a predictor of disease severity among Covid-19  
469 patients: a prospective cohort study. *BMC Infect. Dis.* **23**, 311 (2023).
- 470 17. Dhar, M. S. *et al.* Genomic characterization and epidemiology of an emerging SARS-CoV-2 variant  
471 in Delhi, India. *Science* **374**, 995–999 (2021).
- 472 18. Santa Cruz, A. *et al.* Interleukin-6 Is a Biomarker for the Development of Fatal Severe Acute  
473 Respiratory Syndrome Coronavirus 2 Pneumonia. *Front. Immunol.* **12**, (2021).
- 474 19. Korobova, Z. R. *et al.* A Comparative Study of the Plasma Chemokine Profile in COVID-19 Patients  
475 Infected with Different SARS-CoV-2 Variants. *Int. J. Mol. Sci.* **23**, 9058 (2022).
- 476 20. Lorè, N. I. *et al.* CXCL10 levels at hospital admission predict COVID-19 outcome: hierarchical  
477 assessment of 53 putative inflammatory biomarkers in an observational study. *Mol. Med.* **27**, 129 (2021).
- 478 21. van der Ploeg, K. *et al.* TNF- $\alpha$ + CD4+ T cells dominate the SARS-CoV-2 specific T cell response in  
479 COVID-19 outpatients and are associated with durable antibodies. *Cell Rep. Med.* **3**, 100640 (2022).
- 480 22. Liu, Q. Q. *et al.* Cytokines and their relationship with the severity and prognosis of coronavirus  
481 disease 2019 (COVID-19): a retrospective cohort study. *BMJ Open* **10**, e041471 (2020).
- 482 23. Schultz-Cherry, S. *et al.* Cross-reactive Antibody Response to mRNA SARS-CoV-2 Vaccine After  
483 Recent COVID-19-Specific Monoclonal Antibody Therapy. *Open Forum Infect. Dis.* **8**, ofab420 (2021).
- 484 24. Tang, L. *et al.* Host Predictors of Broadly Cross-Reactive Antibodies Against Severe Acute  
485 Respiratory Syndrome Coronavirus 2 (SARS-CoV-2) Variants of Concern Differ Between Infection and  
486 Vaccination. *Clin. Infect. Dis. Off. Publ. Infect. Dis. Soc. Am.* **75**, e705–e714 (2022).

- 487 25. Lin, C.-Y. *et al.* Pre-existing humoral immunity to human common cold coronaviruses negatively  
488 impacts the protective SARS-CoV-2 antibody response. *Cell Host Microbe* **30**, 83-96.e4 (2022).
- 489 26. Horton, R. E. & Vidarsson, G. Antibodies and Their Receptors: Different Potential Roles in Mucosal  
490 Defense. *Front. Immunol.* **4**, 200 (2013).
- 491 27. Yoshida, M. *et al.* IgG transport across mucosal barriers by neonatal Fc receptor for IgG and  
492 mucosal immunity. *Springer Semin. Immunopathol.* **28**, 397–403 (2006).
- 493 28. Woof, J. M. & Russell, M. W. Structure and function relationships in IgA. *Mucosal Immunol.* **4**,  
494 590–597 (2011).
- 495 29. Wright, P. F. *et al.* Longitudinal Systemic and Mucosal Immune Responses to SARS-CoV-2  
496 Infection. *J. Infect. Dis.* **226**, 1204–1214 (2022).
- 497 30. Guerrieri, M. *et al.* Nasal and Salivary Mucosal Humoral Immune Response Elicited by mRNA  
498 BNT162b2 COVID-19 Vaccine Compared to SARS-CoV-2 Natural Infection. *Vaccines* **9**, 1499 (2021).
- 499 31. Santos, J. de M. B. dos *et al.* In Nasal Mucosal Secretions, Distinct IFN and IgA Responses Are  
500 Found in Severe and Mild SARS-CoV-2 Infection. *Front. Immunol.* **12**, (2021).
- 501 32. Crescenzo-Chaigne, B. *et al.* Nasopharyngeal and serological anti SARS-CoV-2 IgG/IgA responses  
502 in COVID-19 patients. *J. Clin. Virol. Plus* **1**, 100041 (2021).
- 503 33. Zervou, F. N. *et al.* SARS-CoV-2 antibodies: IgA correlates with severity of disease in early COVID-  
504 19 infection. *J. Med. Virol.* **93**, 5409–5415 (2021).
- 505 34. Hansen, C. B. *et al.* SARS-CoV-2 Antibody Responses Are Correlated to Disease Severity in COVID-  
506 19 Convalescent Individuals. *J. Immunol.* **206**, 109–117 (2021).
- 507 35. Vidarsson, G., Dekkers, G. & Rispens, T. IgG Subclasses and Allotypes: From Structure to Effector  
508 Functions. *Front. Immunol.* **5**, (2014).
- 509 36. Robert-Guroff, M. IgG surfaces as an important component in mucosal protection. *Nat. Med.* **6**,  
510 129–130 (2000).
- 511 37. Sajadi, M. M. *et al.* Mucosal and Systemic Responses to Severe Acute Respiratory Syndrome  
512 Coronavirus 2 Vaccination Determined by Severity of Primary Infection. *mSphere* **7**, e00279-22 (2022).
- 513 38. Sterlin, D. *et al.* IgA dominates the early neutralizing antibody response to SARS-CoV-2. *Sci. Transl.*  
514 *Med.* **13**, eabd2223 (2021).
- 515 39. Wohlgemuth, N. *et al.* An Assessment of Serological Assays for SARS-CoV-2 as Surrogates for  
516 Authentic Virus Neutralization. *Microbiol. Spectr.* **9**, e0105921 (2021).

517

518

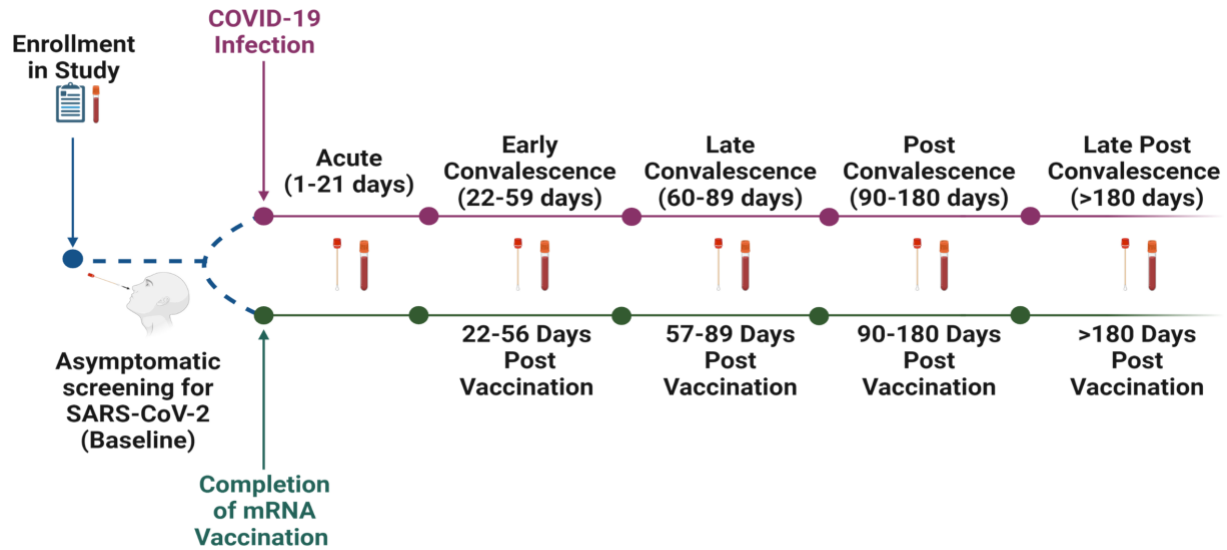
519

520 **Figures and Tables**

521 **Table 1. Cohort characteristics.** The age range, sex distribution, race, and ethnicity of individuals in the  
 522 infected (n=48) and vaccinated (n=26) cohorts. IQR stands for inter-quartile range with the first and third  
 523 quartiles listed.

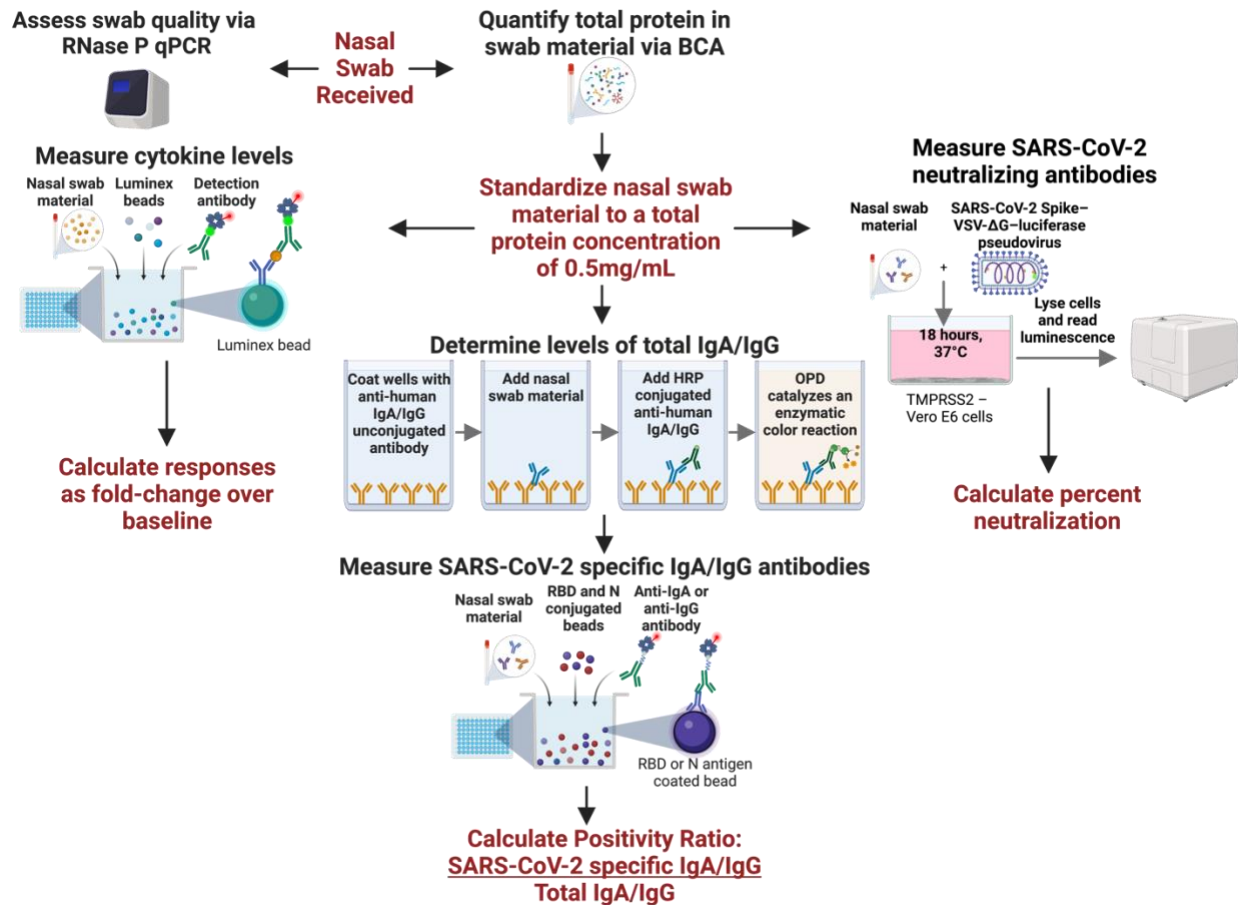
Characteristic		Infection (n=48)	Vaccinated (n=26)
<b>Age (Median [IQR])</b>		43.00 [34.25, 53.00]	41.00 [34.00, 55.75]
<b>Sex (%)</b>	Female	40 (83.3)	18 (69.2)
	Male	8 (16.7)	8 (30.8)
<b>Race (%)</b>	Asian	1 (2.1)	4 (15.4)
	Black/African American	12 (25.0)	3 (11.5)
	WhiteCaucasian	35 (72.9)	19 (73.1)
<b>Ethnicity (%)</b>	Hispanic	1 (2.1)	0 (0.0)
	Non-Hispanic	40 (83.3)	23 (88.5)
	Other, Non-Hispanic	7 (14.6)	3 (11.5)

524



525

526 **Fig. 1. Study timeline.** Individuals enrolled in the SJTRC study in early 2020. Upon enrollment, a blood  
527 sample and demographic information were collected followed by collection of weekly nasopharyngeal  
528 swabs as a part of a SARS-CoV-2 employee asymptomatic screening program. If someone tested positive  
529 prior to becoming vaccinated, they were included in the infected cohort. After testing positive, nasal  
530 swabs and plasma were collected during the acute, early convalescent, late convalescent, post  
531 convalescent, and late post convalescent phases of infection. If individuals managed to remain SARS-CoV-  
532 2 negative before receiving two doses of the Pfizer mRNA BNT162b2 vaccine, they were included in the  
533 vaccination cohort. These individuals also provided nasal swabs and plasma at 22-56 days post vaccination  
534 (dpv), 57-89 dpv, 90-180 dpv, and >180 dpv.



535

536 **Fig. 2. Methodology for measuring innate and adaptive mucosal immune responses from a single nasal**

537 **swab.** Upon receipt, nasal swabs were thawed and aliquoted. One aliquot was used to assess swab quality

538 by the presence of RNase P. A second aliquot was used to determine total protein concentration using

539 BCA. Nasal swabs were diluted to a standardized concentration of 0.5mg/mL for downstream assays to

540 account for the differences in total protein. Cytokines were measured using a Luminex kit with

541 streptavidin-PE conjugated detection antibody. We reported cytokine values as a fold-change over

542 baseline. We determined total IgA and IgG levels using an ELISA with anti-human IgA or IgG as a capture

543 antibody. A second, HRP-conjugated, anti-human IgA or IgG was used to detect IgA or IgG captured from

544 nasal swab samples. The total peak area under the curve was calculated and used as the variable for total

545 IgA or IgG levels. SARS-CoV-2 specific antibodies were measured using a Luminex based kit with

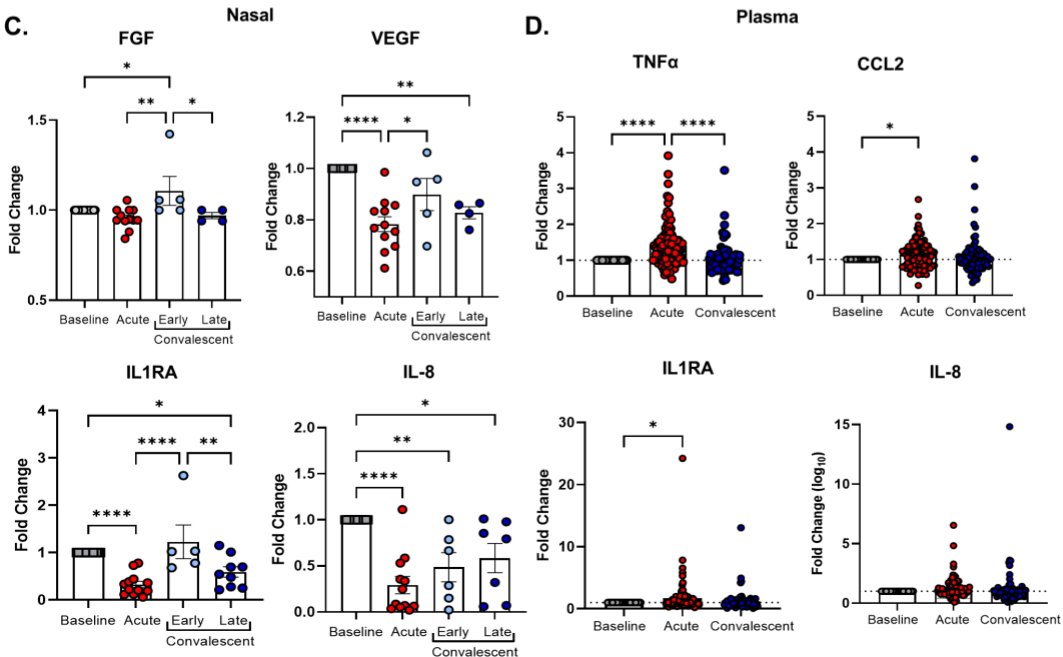
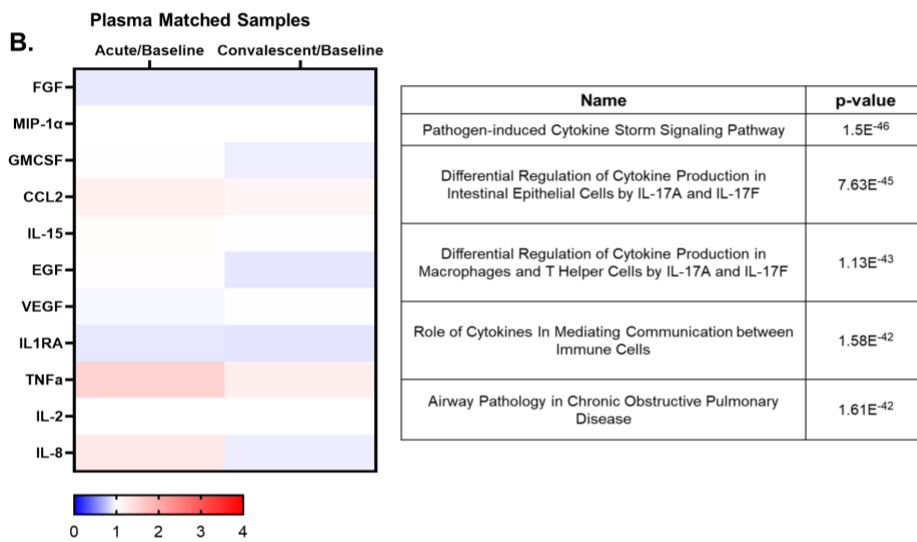
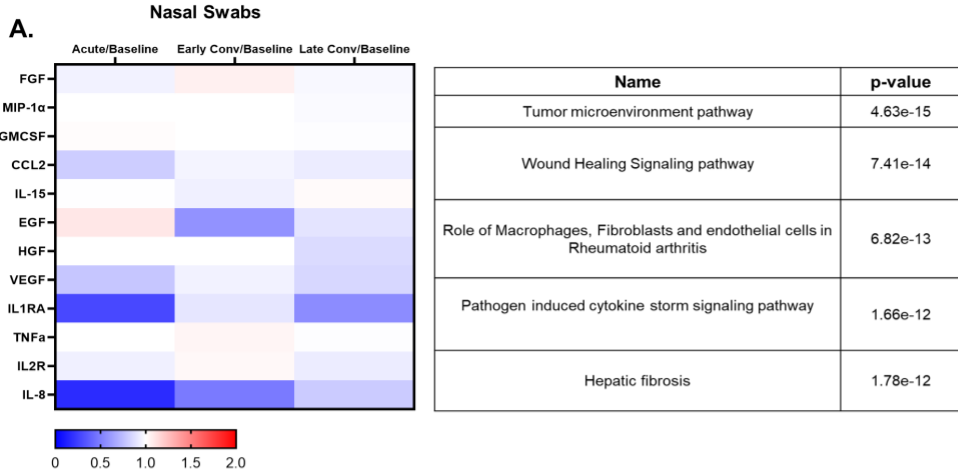
546 streptavidin-PE conjugated anti-human IgA or IgG secondary antibodies. A “positivity ratio” was calculated

547 by dividing antigen specific IgA/IgG by total IgA/IgG. Neutralizing antibodies were determined using a

548 SARS-CoV-2 Spike-VSV-ΔG- luciferase pseudovirus. Nasal swab material was incubated with the virus for

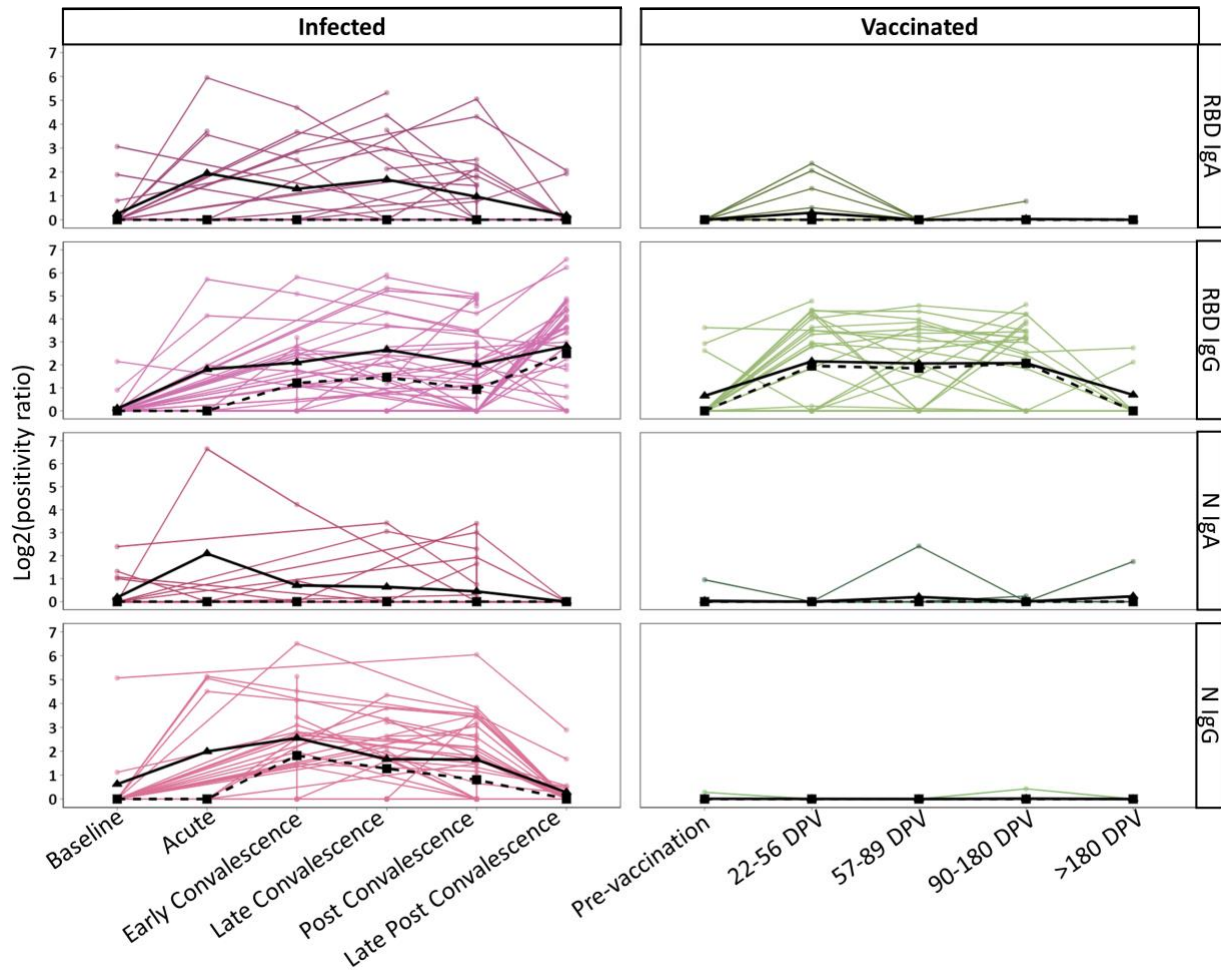
549 1 hour prior to infecting confluent TMPRSS2 cells. The following day, cells were lysed and luminescence

550 was measured. Percent neutralization was calculated for each swab by comparing the nasal swab + virus  
551 luminescence to virus only luminescence.



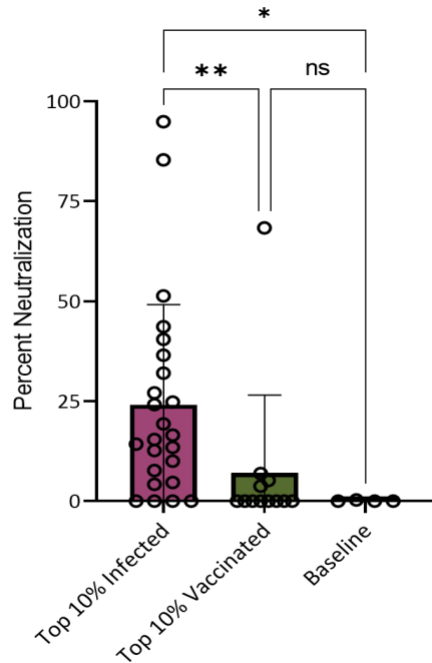


553 **Fig. 3. SARS-CoV-2 infection alters cytokine responses differentially in the plasma and nasal cavity over**  
554 **time.** Nasal swabs or plasma samples were collected at various times-post testing positive for SARS-CoV-  
555 2 and a baseline sample for nasal and plasma pre-infection was used for normalization. Cytokines were  
556 assessed by multiplex Luminex assay. **(A, B)** Heat map of the median cytokine fold changes response to  
557 each person's baseline value to account for human variation for nasal swabs **(A)** or plasma samples **(B)**.  
558 Convalescent stage was split into early (days 21-62) and late (>62 days) post-infection to study the  
559 longitudinal impact of SARS-CoV-2 infection on mucosal cytokine responses **(A)**. Ingenuity pathway  
560 analyses using predetermined signaling pathways on cytokines that were up or downregulated were  
561 assessed for both the nasal and plasma **(A, B)**. **(C)** Fold change from baseline in acute, early, or late  
562 convalescent for cytokines FGF, VEGF, IL1RA, and IL-8 from nasal swabs. **(D)** Fold change from baseline in  
563 acute or convalescent from plasma for TNF $\alpha$ , CCL2, IL1RA, and IL-8. Heat maps and subsequent statistical  
564 analyses were conducted in GraphPad Prism version 9. Statistical analyses include a One-way ANOVA with  
565 Tukey's Multiple Comparisons test **(D)**. \*  $p < .05$ , \*\*  $p < .01$ , \*\*\*  $p < .001$ , \*\*\*\*  $p < .0001$ . Plasma, n=96  
566 for baseline, acute and convalescent; nasal swabs, n=28 (baseline), n=12 (acute), and n=21 (total early +  
567 late convalescent). Note, not all individuals had cytokine levels detected in the nasal cavity at baseline or  
568 post-infection, which were excluded from this analysis.



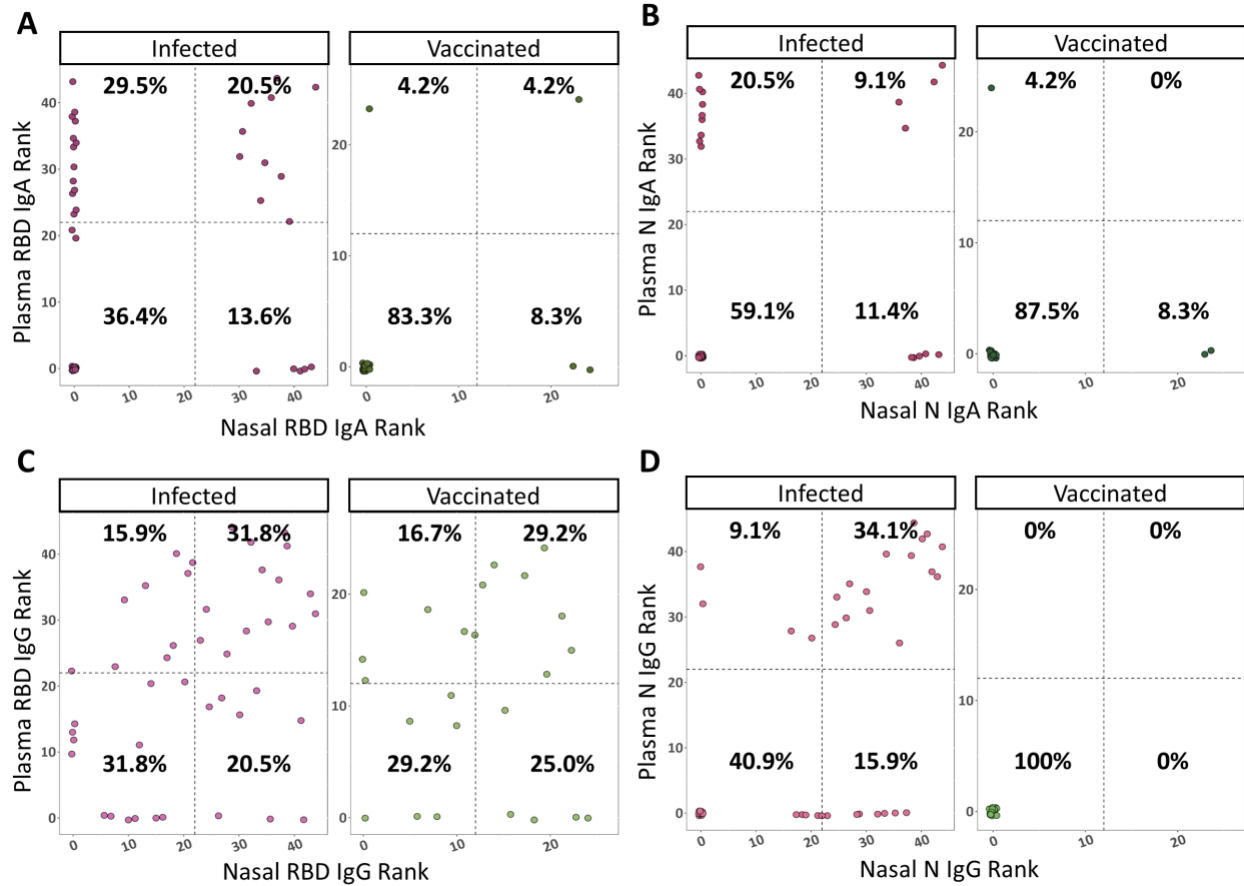
569

570 **Fig. 4. Longitudinal kinetics of mucosal anti-SARS-CoV-2 IgA and IgG in infected and vaccinated**  
571 **individuals.** The responses of infected (left) and vaccinated individuals (right) are shown. Positivity ratios  
572 are shown for anti-RBD IgA, anti-RBD IgG, anti-N IgA, and anti-N IgG. Collection timepoints are listed for  
573 each cohort as either a phase of infection or days post vaccination (DPV). The solid black line on each  
574 graph represents the mean response and the dotted line represents the median response at each time  
575 point.



576

577 **Fig. 5. Neutralization activity is higher in nasal swabs from infected individuals.** Nasal swabs with the  
578 top 10% anti-RBD IgA and IgG positivity ratios were selected for neutralization assays. Percent  
579 neutralization of the swab material at a concentration of 0.5mg/mL total protein is shown. For the infected  
580 cohort N=24, for the vaccinated cohort N=12, and a final N of 4 of baseline samples was included. Each  
581 sample was run in duplicate. One baseline sample was removed prior to statistical analyses after being  
582 identified as an outlier through a ROUT test in PRISM 9. Kruskal-Wallis multiple comparisons were used  
583 to detect significant differences between groups. \*Indicates P=0.0299, \*\*indicates P=0.0057, and ns  
584 stands for non-significant.



585

586 **Fig. 6. Anti-SARS-CoV-2 responses have compartmental bias.** Each person's longitudinal nasal and plasma  
 587 response was summarized using AUC analyses, calculated using R software. AUCs were ranked from  
 588 lowest to highest, with the highest rank indicating the best response. Individuals with no response were  
 589 given a rank of 0. These ranks are presented in scatterplots, with the dotted lines dividing them into 4  
 590 quadrants representing high plasma responses (top right), high nasal and plasma responses (top left), high  
 591 nasal responses (bottom right), and low responders (bottom left). The percentage of people within each  
 592 quadrant is listed on the graphs. **(A)** Plasma vs nasal anti-RBD IgA ranks. **(B)** Plasma vs nasal anti-N IgA  
 593 ranks. **(C)** Plasma vs nasal anti-RBD IgG ranks. **(D)** Plasma vs nasal anti-N IgG ranks.